Time-Averaged Probabilistic Model for Irregular Wave Runup on Permeable Slopes

Nobuhisa Kobayashi[1]; Francisco J. de los Santos[2]; and Peter G. Kearney[3]

Abstract: A time-averaged probabilistic model is developed to predict irregular wave runup statistics on permeable slopes such as cobble beaches and revetments. The cross-shore variations of the mean and standard deviation of the free surface elevation and horizontal fluid velocities above and inside a porous layer are predicted using the time-averaged continuity, momentum, and energy equations. The mean and standard deviation of the shoreline elevation measured by a runup wire are estimated from the predicted mean and standard deviation of the free surface elevation. The wave runup height above the mean water level, including wave setup, is assumed to be given by the Rayleigh distribution. The wave reflection coefficient is estimated from the wave energy flux remaining at the still water shoreline. This computationally efficient model is shown to be in fair agreement with 57 small-scale tests conducted on 1/5 and 1/2 permeable slopes situated inside surf zones on impermeable gentle slopes.

DOI: 10.1061/(ASCE)0733-950X(2008)134:2(88)

CE Database subject headings: Wave runup; Beaches; Shoaling; Wave reflection; Slopes; Probability.

Introduction

The prediction of irregular wave runup is necessary in determining the crest height of a coastal structure and the landward limit of wave action on a beach. A large number of studies were performed to understand the swash dynamics and predict wave runup for given slope and offshore wave characteristics, as reviewed by Kobayashi (1999). The prediction of wave runup was initially based on experiments and empirical formulas because of the complexity involved in wave breaking and runup. Time-dependent numerical models for shallow-water waves were developed to predict regular wave runup (Kobayashi et al. 1987), irregular wave runup on a rough impermeable slope (Kobayashi et al. 1990), and irregular wave runup on a permeable slope (Wurjanto and Kobayashi 1993). These models are one dimensional in the cross-shore direction and do not predict the vertical variations of fluid velocities. Vertically two-dimensional models were also developed to predict plunging waves on an impermeable slope (van der Meer et al. 1993) and regular wave interaction with a steep porous structure (Liu et al. 1999). These numerical models predict the detailed temporal and spatial variations of the free surface elevation and fluid velocities which are needed to understand the complicated hydrodynamics.

For practical applications, the time-dependent models for wave runup have not been applied routinely perhaps because these models require significant computational efforts and experience to run computer programs and obtain quantities of practical importance. On the other hand, empirical formulas for irregular wave runup on coastal structures have been improved to account for various factors (van der Meer and Janssen 1995; van Gent 2001) but are not versatile enough to deal with various combinations of different beaches and structures. These empirical formulas require the input of the representative height and period of incident waves at the toe of the structure which is normally located inside the surf zone during a severe storm. Consequently, a wave model will be necessary to predict the wave transformation from offshore to the toe of the structure.

Irregular wave breaking and wave setup on an impermeable beach of arbitrary profile are generally predicted using numerical models such as that of Battjes and Stive (1985) based on time-averaged momentum and energy equations. Their time-averaged model predicts only the mean and standard deviation of the free surface elevation but is widely used because of its computational efficiency. In this study, the time-averaged model of Battjes and Stive (1985) is extended landward to a permeable slope such as a revetment and a static cobble beach. The extended wave propagation model is combined with a probabilistic wave runup model to predict the runup heights of practical importance such as the significant and 2% runup heights. Furthermore, this time-averaged probabilistic model predicts the cross-shore variations of the mean and standard deviation of the free surface elevation and horizontal fluid velocities above and inside the permeable layer.

In the following, the time-averaged probabilistic model is presented first. The laboratory experiments using 1/5 and 1/2 permeable slopes are described second. The developed model is compared with 57 tests in the two experiments and used to examine the permeability effects on the wave motion on the slope. Finally, the findings of this study are summarized.

[1]Professor and Director, Center for Applied Coastal Research, Univ. of Delaware, Newark, DE 19716 (corresponding author). E-mail: nk@coastal.udel.edu

[2]Ph.D. Candidate, Grupo de Puertos y Costas, E.T.S.I. Caminos, Canales y Puertos, Univ. de Granada, CEAMA, Avda. del Mediterraneo s/n, 18006 Granada, Spain.

[3]Project Manager, Duffield Associates, Inc., 5400 Limestone Rd. Wilmington, DE 19808.

Note. Discussion open until August 1, 2008. Separate discussions must be submitted for individual papers. To extend the closing date by one month, a written request must be filed with the ASCE Managing Editor. The manuscript for this paper was submitted for review and possible publication on May 31, 2005; approved on May 18, 2007. This paper is part of the ***Journal of Waterway, Port, Coastal, and Ocean Engineering***, Vol. 134, No. 2, March 1, 2008. ©ASCE, ISSN 0733-950X/2008/2-88–96/$25.00.

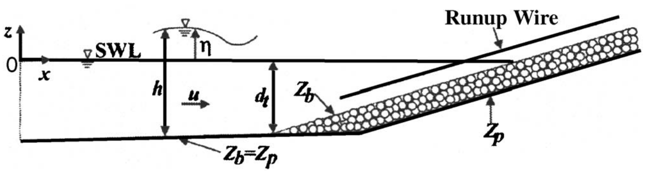

Fig. 1. Time-averaged model for wave propagation on permeable slope

Time-Averaged Probabilistic Model

The problem examined here is depicted in Fig. 1 where the beach slope and permeable slope are arbitrary. Alongshore uniformity and normally incident waves are assumed. The cross-shore coordinate x is positive onshore. The vertical coordinate z is positive upward with $z=0$ at the still water level (SWL). The upper and lower boundaries of the permeable stone layer are located at $z=z_b$ and z_p, respectively, where the lower boundary is assumed impermeable to simplify the problem. The gently sloping beach in front of the permeable steep slope is assumed to be impermeable and $z_b=z_p$ on the beach. The instantaneous water depth and free surface elevation are denoted by h and η, respectively, and $h=(\eta-z_b)$. The horizontal fluid velocity u=depth-averaged velocity. The still water depth at the toe of the permeable slope denoted by d_t is arbitrary but is normally located inside the surf zone during storms.

The time-averaged continuity, momentum, and energy equations used here are those given by Kobayashi et al. (2007) for the prediction of irregular breaking wave transmission over a submerged porous breakwater. These conservation equations are applicable for the case of negligible reflected waves. The time-averaged momentum and energy equations are expressed as

$$\frac{dS_{xx}}{dx}=-\rho g\bar{h}\frac{d\bar{\eta}}{dx}-\tau_b;\quad \frac{dF}{dx}=-D_B-D_f-D_r \tag{1}$$

where S_{xx}=cross-shore radiation stress; ρ=fluid density; g=gravitational acceleration; $\bar{h}$=mean water depth with the overbar denoting time averaging; $\bar{\eta}$=wave setup or setdown; τ_b=time-averaged bottom shear stress; F=wave energy flux per unit width; and D_B, D_f and D_r=time-averaged energy dissipation rate per unit horizontal area due to wave breaking, bottom friction, and porous flow resistance, respectively.

Linear wave theory for onshore progressive waves is used to estimate S_{xx} and F where the root-mean-square wave height H_{rms} for irregular wave energy used by Battjes and Stive (1985) is defined as $H_{\text{rms}}=\sqrt{8}\ \sigma_\eta$ with σ_η=standard deviation of η

$$S_{xx}=\rho g\sigma_\eta^2(2n-0.5);\quad F=\rho gC_g\sigma_\eta^2 \tag{2}$$

where $n=C_g/C_p$ with C_g and C_p=group velocity and phase velocity in the mean water depth $\bar{h}$ corresponding to the spectral peak period T_p of incident waves.

The bottom shear stress τ_b and the corresponding dissipation rate D_f are expressed using the formulas based on the quadratic drag force based on the horizontal velocity u. The mean and standard deviation of u are denoted by $\bar{u}$ and σ_u, respectively. The Gaussian distribution of u and the equivalency of the time and probabilistic averaging are assumed to express τ_b and D_f in terms of $\bar{u}$ and σ_u

$$\tau_b=\frac{1}{2}\rho f_b\sigma_u^2G_2(u*);\quad D_f=\frac{1}{2}\rho f_b\sigma_u^3G_3(u*);\quad u*=\frac{\bar{u}}{\sigma_u} \tag{3}$$

where f_b=bottom friction factor. The values of $f_b=0$ on the smooth slope and $f_b=0.01$ on the stone slope calibrated by Kobayashi et al. (2007) are used without additional calibration for the present experiments. The analytical functions $G_2(r)$ and $G_3(r)$ for the arbitrary variable r are given by Kobayashi et al. (2005) and can be approximated as $G_2\simeq 1.64r$ and $G_3\simeq(1.6+2.6r^2)$ for $|r|<1$.

The standard deviation σ_u is estimated using the relationship between σ_u and σ_η based on linear shallow-water wave theory (Kobayashi et al. 1998)

$$\sigma_u=\sigma*(g\bar{h})^{0.5};\quad \sigma*=\sigma_\eta/\bar{h} \tag{4}$$

The mean $\bar{u}$ is estimated using the time-averaged, vertically integrated continuity equation $(\sigma_u\sigma_\eta+\bar{u}\bar{h}+\bar{v}h_p)=0$ with the condition of no net landward water flux in the absence of wave overtopping. In this equation, $\sigma_u\sigma_\eta$=onshore flux due to linear shallow-water waves (Kobayashi et al. 1998); $\bar{u}\bar{h}$=offshore flux due to the return current $\bar{u}$; and $\bar{v}h_p$=water flux inside the permeable layer of vertical height h_p due to the time-averaged horizontal discharge velocity $\bar{v}$. Substitution of Eq. (4) into the continuity equation yields

$$\bar{u}=-[\sigma_*^2(g\bar{h})^{0.5}+\bar{v}h_p/\bar{h}];\quad h_p=z_b-z_p \tag{5}$$

where $h_p=0$ on the impermeable beach.

The energy dissipation rate D_r in Eq. (1) is estimated using the formula by Wurjanto and Kobayashi (1993) based on the discharge velocity v inside the permeable layer as explained by Kobayashi et al. (2007). The laminar and turbulent flow resistance coefficients are estimated using the formulas by van Gent (1995). The input required for these formulas includes n_p=porosity of the stone; D_{n50}=nominal stone diameter defined as $D_{n50}=(M_{50}/\rho_s)^{1/3}$ with M_{50}=median stone mass and ρ_s=stone density; and ν=kinematic viscosity of water ($\nu\simeq 0.01\ \text{cm}^2/\text{s}$). The mean $\bar{v}$ and standard deviation σ_v of the discharge velocity are estimated assuming the local force balance between the horizontal gradient of hydrostatic pressure and the flow resistance inside the permeable layer (Kobayashi et al. 2007).

The energy dissipation rate D_B due to wave breaking in Eq. (1) is estimated using the formula by Battjes and Stive (1985) modified by Kobayashi et al. (2007) to increase D_B in the region where the horizontal length scale is imposed by the small depth and bottom slope. The formula by Battjes and Stive (1985) includes the empirical breaker ratio parameter γ. Their calibrated values of γ were in the range of 0.6–0.8. In the subsequent comparisons, γ=0.6, 0.7, and 0.8 are tried.

Eqs. (1)–(5) are solved using a finite difference method with constant nodal spacing Δx of approximately 1 cm for a sufficient resolution near the shoreline in the following small-scale experiments. The bottom elevation $z_b(x)$ and the impermeable boundary $z_p(x)$ are specified as input. The stone is characterized by its nominal diameter D_{n50} and porosity n_p. The measured values of $T_p, \bar{\eta}$ and $H_{\text{rms}}=\sqrt{8}\sigma_\eta$ are specified at the seaward boundary $x=0$ outside the surf zone. The landward-marching computation is continued until the computed value of $\bar{h}$ or σ_η becomes negative in the region of $\bar{h}$ on the order of 0.1 cm. The computation time is of the order of 1 s using a workstation.

The time-averaged model based on Eqs. (1)–(5) neglects reflected waves. An attempt is made to estimate the degree of wave reflection. The onshore energy flux F in Eq. (1) decreases land-

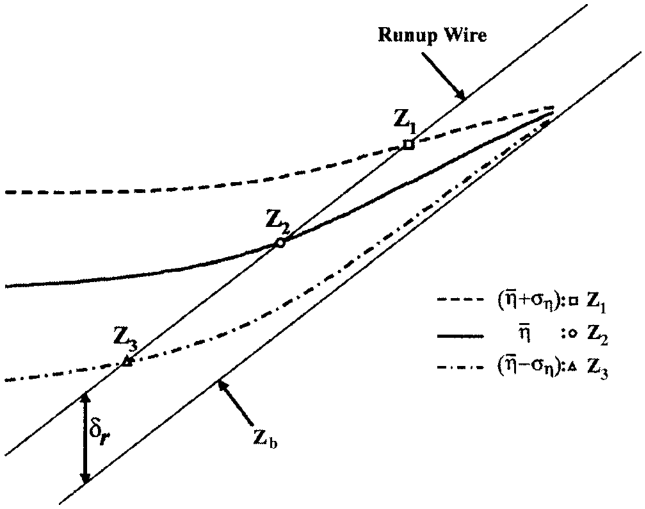

Fig. 2. Elevations Z_1, Z_2, and Z_3 of intersections of $(\bar{\eta}+\sigma_\eta)$, $\bar{\eta}$ and $(\bar{\eta}-\sigma_\eta)$ with runup wire where $\bar{\eta}$ and σ_η are mean and standard deviation of free surface elevation

ward due to energy dissipation caused by wave breaking, bottom friction, and flow resistance inside the permeable slope. The residual energy flux F_{sws} at the still water shoreline located at $z_b=0$ is assumed to be reflected from the slope and propagate seaward. The effect of reflected waves on the incident waves may be neglected if F_{sws} is small in comparison to the incident wave energy flux. The root-mean-square wave height $(H_{\mathrm{rms}})_r$ due to the reflected wave energy flux is crudely estimated as

$$(H_{\mathrm{rms}})_r = [8F_{\mathrm{sws}}/(\rho g C_g)]^{0.5} \tag{6}$$

A probabilistic model for irregular wave runup is developed using the computed $\bar{\eta}(x)$ and $\sigma_\eta(x)$ on the permeable slope. A runup wire is used in the subsequent experiments to measure the shoreline oscillations above the slope as shown in Fig. 1. The vertical height δ_r of the wire above the average stone surface is given in the following. The wire measures the instantaneous elevation $\eta_r(t)$ above SWL of the intersection between the wire and the free surface unlike a wave gauge that measures $\eta(t)$ at given x. Fig. 2 depicts an intuitive method used to estimate the mean $\bar{\eta}_r$ and standard deviation σ_r of $\eta_r(t)$. The probabilities of η exceeding $(\bar{\eta}+\sigma_\eta)$, $\bar{\eta}$ and $(\bar{\eta}-\sigma_\eta)$ are assumed to be the same as the probabilities of η_r exceeding $(\bar{\eta}_r+\sigma_r)$, $\bar{\eta}_r$, and $(\bar{\eta}_r-\sigma_r)$, respectively. The elevations of Z_1, Z_2, and Z_3 of the intersections of $(\bar{\eta}+\sigma)$, $\bar{\eta}$ and $(\bar{\eta}-\sigma)$ with the runup wire are obtained using the computed $\bar{\eta}(x)$ and $\sigma(x)$ together with the wire elevation $[z_b(x)+\delta_r]$. The obtained elevations are assumed to correspond to $Z_1=(\bar{\eta}_r+\sigma_r)$, $Z_2=\bar{\eta}_r$, and $Z_3=(\bar{\eta}_r-\sigma_r)$. The mean and standard deviation of $\eta_r(t)$ are estimated as

$$\bar{\eta}_r = (Z_1+Z_2+Z_3)/3; \quad \sigma_r = (Z_1-Z_3)/2 \tag{7}$$

where the use of Z_1, Z_2, and Z_3 to estimate $\bar{\eta}_r$ is slightly more reliable than $\bar{\eta}_r=Z_2$ because the elevation Z_2 is somewhat sensitive to the detailed spatial variation of $\bar{\eta}(x)$.

The runup height R is defined as the crest height above SWL of the temporal variation of η_r. The time series of $[\eta_r(t)-\bar{\eta}_r]$ is analyzed using a zero-upcrossing method to identify the crests in the time series. This procedure is the same as that used for the analysis of the wave crests in the time series of $\eta(t)$ except that the wave crest is defined as the height above the mean water level. The probability distribution of linear wave crests is normally given by the Rayleigh distribution (e.g., Goda 2000). As a first approximation, the runup height $(R-\bar{\eta}_r)$ above the mean level $\bar{\eta}_r$ is given by the Rayleigh distribution

$$P(R) = \exp\left[-2\left(\frac{R-\bar{\eta}_r}{R_{1/3}-\bar{\eta}_r}\right)^2\right] \tag{8}$$

where $P(R)$=exceedance probability of the runup height R above SWL; and $R_{1/3}$=significant runup height defined as the average of 1/3 highest values of R. The mean $\bar{\eta}_r$ related to wave setup is normally neglected in Eq. (8) for the prediction of irregular wave runup on steep coastal structures (e.g., van der Meer and Janssen 1995). However, wave setup on gentler slopes is not negligible as will be shown for the permeable slope experiments in this study.

Finally, it is necessary to express $R_{1/3}$ in terms of $\bar{\eta}_r$ and σ_r estimated using Eq. (7). If the probability distribution of η_r is approximately Gaussian, use may be made of $(R_{1/3}-\bar{\eta}_r)\simeq 2\sigma_r$ (Goda 2000). For the following experiments using 1/5 and 1/2 permeable slopes, $R_{1/3}$ is estimated as

$$R_{1/3} = \bar{\eta}_r + (2+\tan\theta)\sigma_r \tag{9}$$

where θ=slope angle from the horizontal and $\tan\theta=1/5$ and 1/2 in the experiments. The slope correction in Eq. (9) is purely empirical and needs to be verified for other slopes.

Experiments

The time-averaged probability model is compared with the permeable slope experiments with $\tan\theta=1/2$ and 1/5 by Kearney and Kobayashi (2001a) and de los Santos and Kobayashi (2005), respectively. It should be noted that the initial attempt by Kearney and Kobayashi (2001a) to develop a probabilistic runup model was not successful. The two experiments are explained concisely in the following.

The experiment by de los Santos and Kobayashi (2005) was conducted in a wave flume that was 33 m long, 0.6 m wide, and 1.5 m high as shown in Fig. 3. An impermeable smooth beach with a 1/34.4 slope was installed in the flume. Angular stone was placed randomly on a 1/5 impermeable slope to simulate an idealized cobble beach. The measured nominal diameter and porosity of the angular stone were D_{n50}=3.4 cm and n_p=0.5, respectively. The vertical thickness of the stone layer was 14 cm. Irregular waves, based on the TMA spectrum, were generated in a burst of 429.6 s using a piston-type wave paddle. The sampling rate was 20 Hz for all the time series measured in the experiment. The initial transient of 20 s in each burst was removed for subsequent data analyses.

Thirty tests were conducted for the 1/5 slope experiment. The still water depth d_t at the toe of the slope was varied from 16.6 to 24.6 cm with an increment of 2 cm. The spectral peak period T_p was approximately 1.5, 2.3, and 3.0 s. The root-mean-square wave height $H_{\mathrm{rms}}=\sqrt{8}\sigma_\eta$ was selected to be as large as feasible without any wave breaking in the vicinity of the wavemaker located in the still water depth $d_h=(d_t+31)$ cm. For the specified d_t and T_p, two tests were performed to check the variability of H_{rms} resulting from the generation of large waves.

For each test, seven capacitance-type wave gauges and a runup wire were used to measure the time series of η and η_r at the locations indicated in Fig. 3 where $x=0$ at wave Gauge 1. The vertical height δ_r of the runup wire above the 1/5 slope was approximately 2 cm. Wave Gauges 1–3 were located immediately outside the surf zone and used to separate the incident and

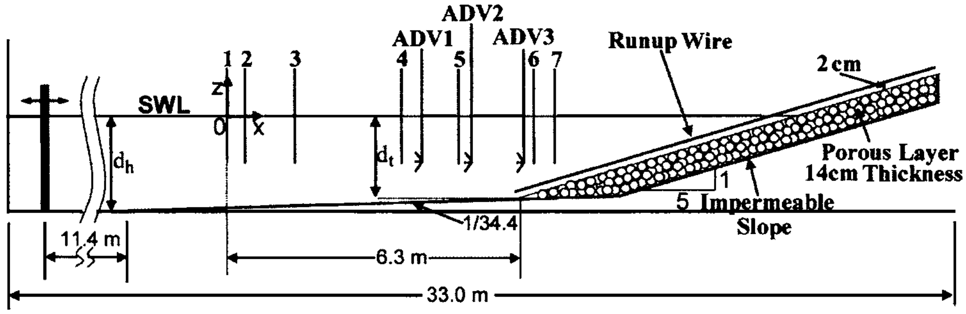

Instrument	1	2	3	4	5	6	7	ADV1	ADV2	ADV3
Location x=[m]	0	0.31	1.31	4.01	5.62	6.59	6.88	4.27	5.91	6.48

Fig. 3. Experimental setup for 1/5 permeable slope

reflected waves using linear wave theory (Kobayashi et al. 1990). The average reflection coefficient r is defined as $r=(H_{\mathrm{rms}})_r/(H_{\mathrm{rms}})_i$ where $(H_{\mathrm{rms}})_r$ and $(H_{\mathrm{rms}})_i$=reflected and incident root-mean-square wave heights. Table 1 shows the ranges of T_p, H_{rms}, and r measured at Wave Gauge 1 for the 30 tests where H_{rms} includes both incident and reflected waves. The difference between H_{rms} and $(H_{\mathrm{rms}})_i$ was less than 5% because $r=0.16-0.24$ and Wave Gauge 1 was located at the horizontal distance of 6.3 m seaward of the toe of the 1/5 slope. Wave Gauges 4–7 measured the irregular breaking wave transformation on the gentle slope and the seaward edge of the 1/5 slope. Three three-dimensional (3D) acoustic Doppler velocimeters (ADVs) were used to measure fluid velocities at the middepth between the still water level and the beach. The cross-shore locations of the three ADVs are given in Fig. 3. The measured vertical and cross-flume velocities appeared to be dominated by turbulent velocities and were much smaller than the cross-shore velocity u which was dominated by the wave component. Only the horizontal velocity u is considered hereafter.

The experiment by Kearney and Kobayashi (2001a) was conducted in a different wave tank that was 30 m long, 2.44 m wide, and 1.5 m high. A plywood beach with a 1/32.1 slope and a stone revetment with a 1/2 slope were installed in the tank. The nominal diameter of the angular stone was $D_{n50}=3.2$ cm and the stone porosity, which was not measured, is assumed to be the same as $n_p=0.5$ for the stone used in the other experiment. The thickness of the permeable layer was approximately 14 cm. This experimental setup corresponded to stone on an earthen slope. A runup wire was placed at a distance of $\delta_r=2.5$ cm above the 1/2 stone revetment. Ten wave gauges were used in this wave tank to measure the irregular wave transformation from outside the surf zone to the toe of the 1/2 slope. Wave Gauge 1 was located 14.8 m seaward of the toe. One ADV was also placed at the toe. Twenty seven tests were conducted for the spectral peak periods $T_p=1.5$, 2.4, and 4.7 s of the TMA spectra and nine different toe depths $d_t=4-20$ cm with an increment of 2 cm. The duration of each test and the sampling rate were 400 s and 20 Hz for $T_p=1.5$ and 2.4 s and 800 s and 10 Hz for $T_p=4.7$ s. The initial transition of 1,200 data points was removed before the data analyses. The ranges of the wave height H_{rms} and the reflection coefficient r at Wave Gauge 1 for the 27 tests are listed in Table 1. The values of r were slightly larger for the 1/2 slope for these two experiments with similar ranges of T_p and H_{rms}.

The probability density functions of the measured $\eta(t)$, $\eta_r(t)$, and $u(t)$ were presented by de los Santos et al. (2005) and Kearney and Kobayashi (2001b) in comparison with the Gaussian and exponential gamma distributions (Kobayashi et al. 1998). The exponential gamma distribution with the measured positive skewness for each time series represents the measured probability density function well. The Gaussian distribution with zero skewness is fair as a first approximation except for the free surface elevation inside the surf zone whose skewness was about unity. It is noted that the Gaussian distributions of u and η_r are assumed for Eqs. (3) and (9). Furthermore, de los Santos et al. (2005) showed that the measured probability distributions of zero-upcrossing wave heights could be represented fairly by the Rayleigh distribution except that the scatter of data points was large for the exceedance probabilities on the order of 0.01.

Fig. 4 compares the measured probability distributions of zero-upcrossing runup heights with the Rayleigh distribution given by Eq. (8) which accounts for the mean $\bar{\eta}_r$ for the runup height R above SWL. Fig. 4 includes all the data points from the 30 and 27 tests in the 1/5 and 1/2 slope experiments. The Rayleigh distribution is a good approximation except for the scatter of data points for small exceedance probabilities partly because the duration of each burst consisted of about 200 waves. The measured probability distributions were also compared with Eq. (8) with $\bar{\eta}_r=0$ (de los Santos and Kobayashi 2005). The agreement is similar for the 1/2 slope but worse for the 1/5 slope because wave setup is not negligible on the 1/5 slope as will be shown later.

Fig. 5 shows the relationship between the 2% runup height $R_{2\%}$ and significant runup height $R_{1/3}$ for each of the 57 tests where Eq. (8) yields

Table 1. Two Experiments with 1/5 and 1/2 Permeable Slopes with Ranges of Toe Depth d_t and Wave Conditions at Wave Gauge 1

Slope	Number of tests	d_t (cm)	T_p (s)	H_{rms} (cm)	r
1/5	30	16.6–24.6	1.5–3.1	7.2–12.2	0.16–0.24
1/2	27	4.0–20.0	1.5–4.7	8.4–16.4	0.20–0.36

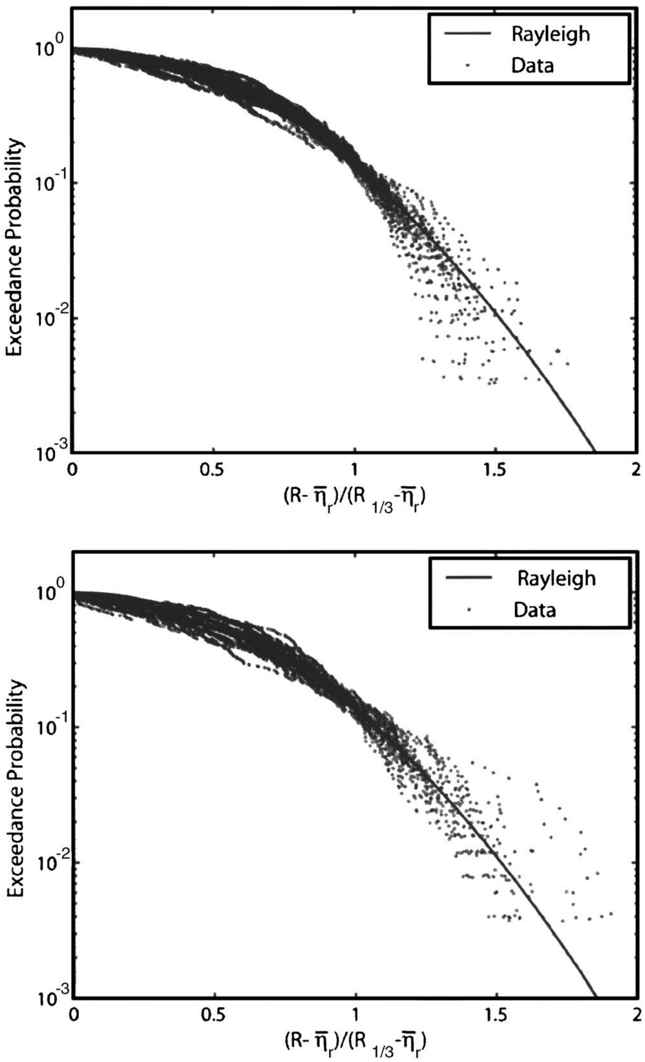

Fig. 4. Measured and Rayleigh exceedance probability distributions of runup height R above SWL for 1/5 (top) and 1/2 (bottom) slope tests

$$R_{2\%}-\bar{\eta}_r=1.4(R_{1/3}-\bar{\eta}_r) \tag{10}$$

It is noted that $R_{2\%}$ is used for the design of the crest height of a dike in The Netherlands (van Gent 2001). Fig. 5 indicates that Eq. (10) based on the Rayleigh distribution with the wave setup effect slightly overpredicts $R_{2\%}$ for given $R_{1/3}$ and $\bar{\eta}_r$. The degree of the overprediction increases when the measured values of $R_{2\%}$ and $R_{1/3}$ are compared with $R_{2\%}=1.4R_{1/3}$ without the wave setup effect (de los Santos and Kobayashi 2005). Fig. 6 examines the accuracy of Eq. (9) for $\tan\theta=1/5$ and 1/2. The slope correction term $(\sigma_r \tan\theta)$ improves the agreement in comparison with $(R_{1/3}-\bar{\eta}_r)=2\sigma_r$ based on the Gaussian probability distribution. This slope correction will not be valid when the slope becomes steeper and the slope angle θ approaches 90°.

Comparisons of Numerical Model with Experiments

Figs. 4–6 indicate that Eqs. (8)–(10) may be used to predict the wave runup heights $R_{1/3}$ and $R_{2\%}$ as well as the value of R for the specified exceedance probability P if the mean $\bar{\eta}_r$ and standard deviation σ_r of the shoreline fluctuations can be predicted accurately by the numerical model. For each of the 57 tests, the bottom profiles $z_b(x)$ and $z_p(x)$ and the measured values of T_p, $\bar{\eta}$ and σ_η at $x=0$ are specified as input to the numerical model. The output of the numerical model includes the cross-shore variations of the variables in Eqs. (1)–(5), and the reflected wave height given by Eq. (6), and the values of $\bar{\eta}_r$ and σ_r in Eq. (7). The only empirical parameter calibrated here is the breaker ratio parameter γ related to D_B in Eq. (1). Use is made of $\gamma=0.7$ calibrated by Kobayashi et al. (2007) who compared the numerical model with the experiment in which the 1/5 permeable slope in Fig. 3 was replaced by a submerged porous breakwater. The increase of γ causes the landward shift of irregular wave breaking on the gently sloping beach. The calibration of γ is made by comparing the

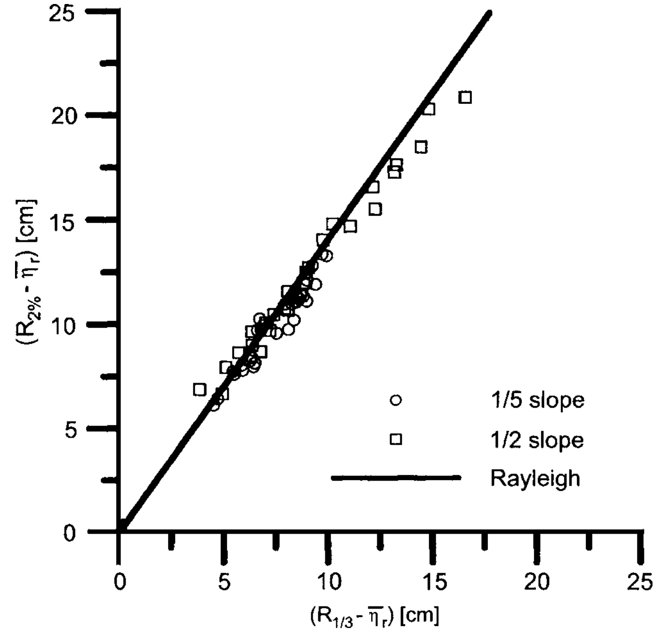

Fig. 5. Relationship between 2% runup height $R_{2\%}$ and significant runup height $R_{1/3}$

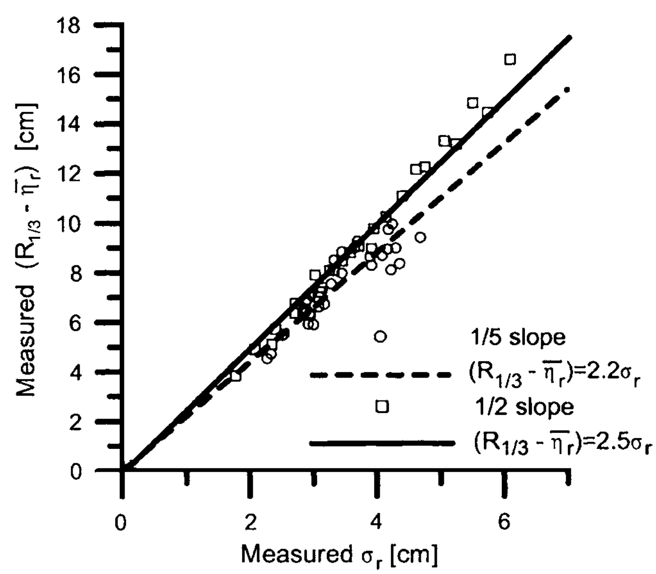

Fig. 6. Empirical formula $(R_{1/3}-\bar{\eta}_r)=2.2\sigma_r$ and $2.5\sigma_r$ for 1/5 and 1/2 slopes

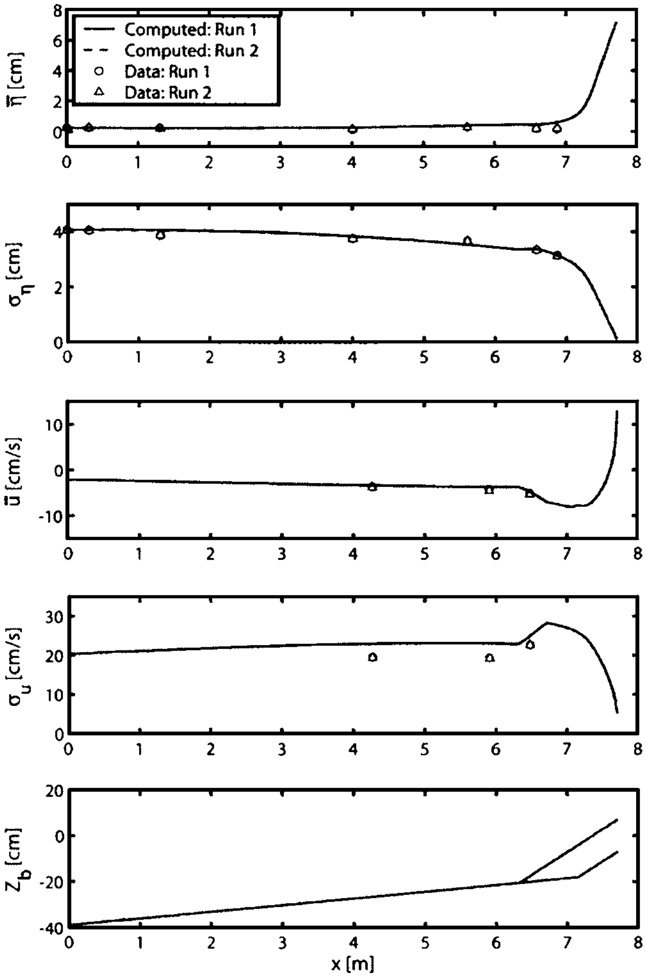

Fig. 7. Measured and predicted cross-shore variations of mean and standard deviation of η and u above bottom profile z_b for two repeated tests on 1/5 slope

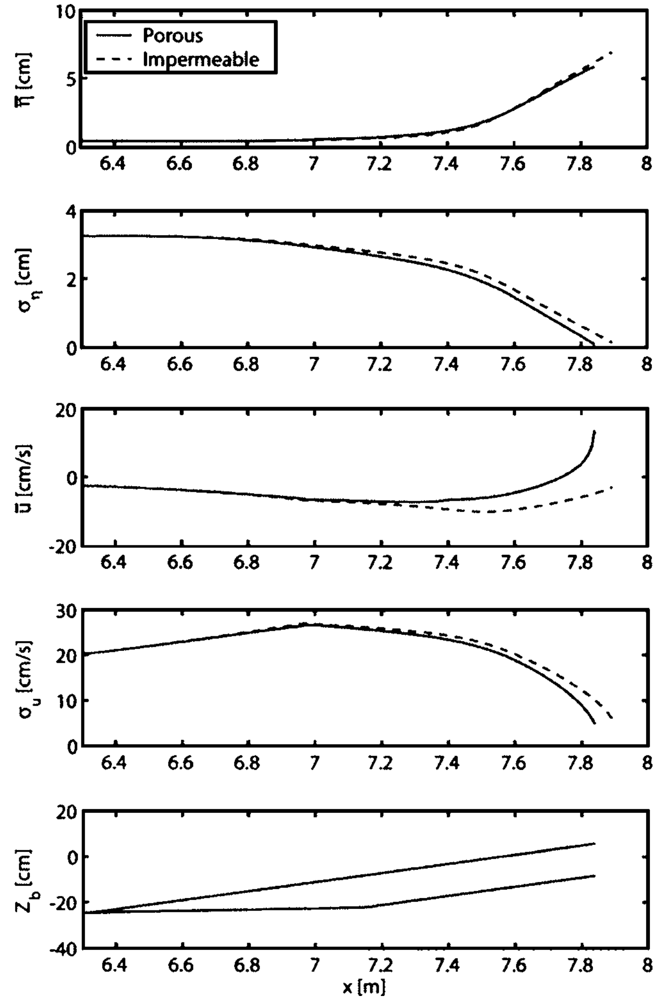

Fig. 8. Permeability effects on $\bar{\eta}$, σ_η, $\bar{u}$, and σ_u

measured and computed cross-shore variations of $\bar{\eta}$, σ_η, $\bar{u}$, and σ_u. The overall agreement is good except for the 1/2 slope tests with T_p=1.5 and 2.4 s. For these tests, γ=0.8 is used to improve the agreement. This indicates the empirical nature of the formula of D_B by Battjes and Stive (1985).

Fig. 7 compares the measured and predicted cross-shore variations of $\bar{\eta}$, σ_η, $\bar{u}$, and σ_u for two repeated tests where $\tan\theta$ =1/5, d_t=20.6 cm, T_p=2.31 s, and H_{rms}=11.46 and 11.49 cm. The landward limit of the bottom profiles $z_b(x)$ and $z_p(x)$ in the bottom panel of Fig. 7 corresponds to that of the computation. The comparisons for the other 14 pairs of repeated tests on the 1/5 slope are presented in the report by de los Santos and Kobayashi (2005). The comparisons for the other pairs are similar to those shown in Fig. 7. The numerical model slightly overpredicts the wave setup $\bar{\eta}$ near the shoreline. The agreement for σ_η is good partly because the measured σ_η did not vary much. The comparisons for $\bar{u}$ and σ_u are somewhat ambiguous because the computed u=depth-averaged velocity but the measured u corresponded to the middepth elevation. The agreement for $\bar{u}$ is better than expected from the previous comparison for a submerged breakwater by Kobayashi et al. (2007). The standard deviation σ_u is overpredicted slightly. On the other hand, the comparisons with the 27 tests in the 1/2 slope experiment were presented in the report by Kearney and Kobayashi (2001a) who used the earlier version of this numerical model by Johnson and Kobayashi (1998). The present numerical model has also been compared with the 27 tests and the difference of the two models is essentially limited to the region near the shoreline where η and u were not measured.

To examine the permeability effects on $\bar{\eta}$, σ_η, $\bar{u}$, and σ_u, computation is also made for the 1/5 slope tests with no permeable layer by specifying $z_p=z_b$ and h_p=0 in Eq. (5). The permeability effects tend to increase with the increase of the toe depth d_t and with the decrease of the period T_p. Consequently, the computed results for the test with the largest d_t=24.6 cm and the smallest T_p=1.59 s are presented in Fig. 8 where H_{rms}=11.59 cm at x=0. The cross-shore variations above the 1/5 slope are shown to differentiate the computed variations on the porous and impermeable slopes shown in the bottom panel of Fig. 8. The wave setup $\bar{\eta}$ reaches a higher elevation as it approaches tangential to the impermeable slope. The standard deviation σ_η decreases landward more gradually because of no energy dissipation due to porous flow resistance. The return current $\bar{u}$ is negative (offshore) on the impermeable slope, whereas $\bar{u}$ becomes positive above the still water shoreline on the porous slope because of infiltration and return flow inside the porous layer. The standard deviation σ_u of the horizontal velocity u above the slope decreases landward more gradually on the impermeable slope.

To interpret the computed variations in Fig. 8, Fig. 9 shows the computed cross-shore variations of $F^*=F/\rho g$, $D_B^*=D_B/\rho g$, $D_r^*=D_r/\rho g$, and $D_f^*=D_f/\rho g$ involved in the energy equation in Eq. (1). The wave energy flux F decreases landward due to the

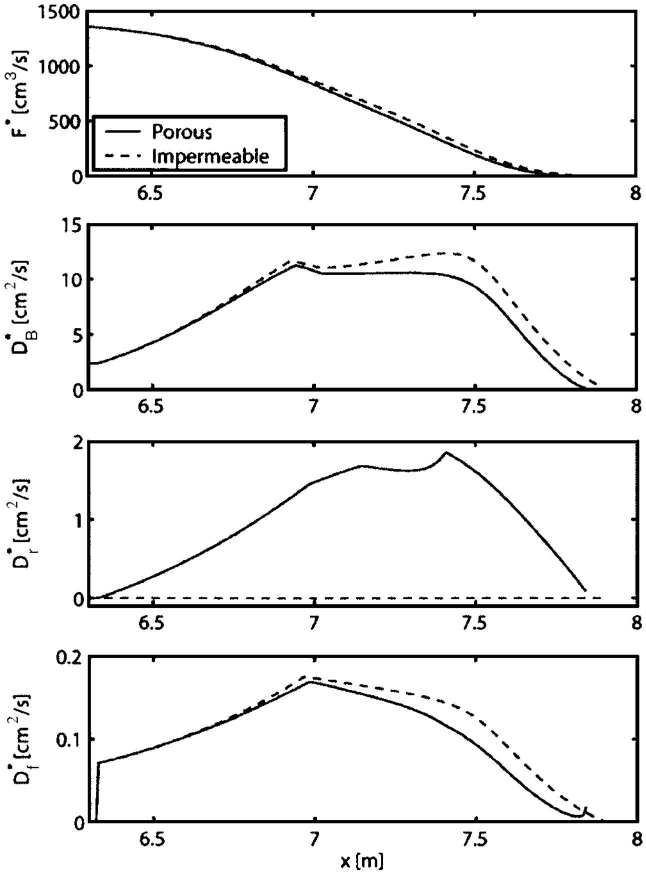

Fig. 9. Permeability effects on wave energy flux $F=\rho g F^*$ and dissipation rates $D_B=\rho g D_B^*$, $D_r=\rho g D_r^*$, and $D_f=\rho g D_f^*$ due to wave breaking, porous flow resistance, and bottom friction, respectively

energy dissipation but the difference between the values on the permeable and impermeable slopes is small for the present experiment with no porous underlayer. The energy dissipation rate D_B due to wave breaking increases on the impermeable slope for which the energy dissipation rate D_r due to porous flow resistance is zero. The energy dissipation rate D_f due to the bottom friction is on the order of 0.02 D_B. The computed results in Figs. 8 and 9 may not be very accurate but indicate the interconnected nature of the variables in Eqs. (1)–(5).

Figs. 10 and 11 compare the measured and predicted values of the mean $\bar{\eta}_r$ and the standard deviation σ_r of the shoreline elevation η_r. The agreement is poor for $\bar{\eta}_r$ on the 1/2 slope. The computed $\bar{\eta}_r$ on the 1/2 slope for $T_p=2.4$ and 4.7 s is too large in comparison with the measured $\bar{\eta}_r$ of about 1 cm where the comparisons for the different values of T_p are presented in the report by de los Santos and Kobayashi (2005). This overprediction does not affect the wave runup heights $R_{1/3}$ and $R_{2\%}$ much because σ_r on the 1/2 slope for $T_p=2.4$ and 4.7 s is of the order of 4 cm and much larger than the measured $\bar{\eta}_r$.

Fig. 12 compares the measured and predicted significant runup heights $R_{1/3}$ where $R_{1/3}$ is predicted using Eq. (9). The numerical model predicts $R_{1/3}$ within the error of about 20% partly because the slope correction is included in Eq. (9) empirically.

Fig. 13 compares the measured, computed and empirical 2% runup heights $R_{2\%}$ where use is made of Eq. (10) for the computed $R_{2\%}$. The empirical formula of van der Meer and Janssen

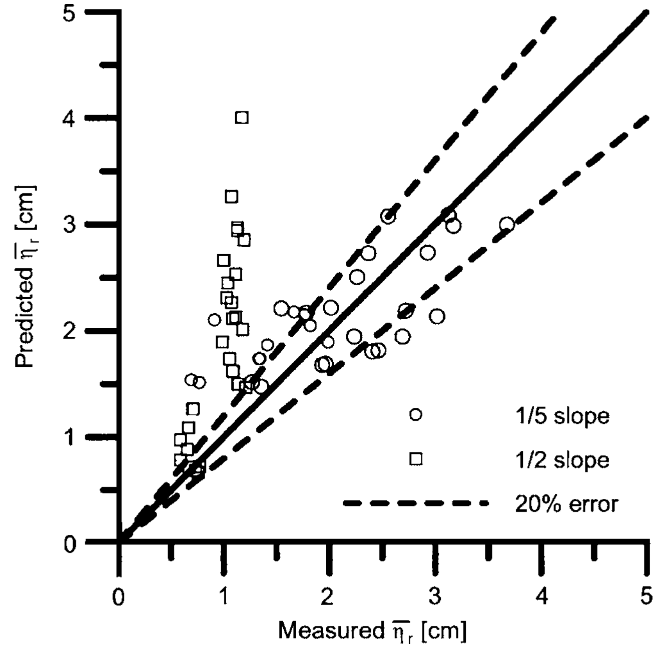

Fig. 10. Measured and predicted mean shoreline elevations $\bar{\eta}_r$

(1995) is also compared with the data. For the case of normally incident waves on a slope with no berm, this formula can be expressed as

$$R_{2\%} = 1.5\xi\gamma_f\gamma_h H_{1/3} \quad \text{with} \quad \xi \leqslant 2 \tag{11}$$

with

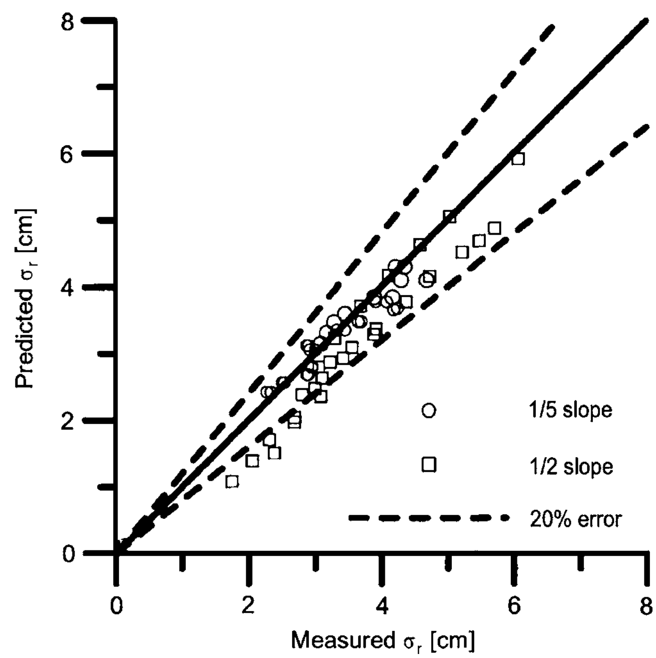

Fig. 11. Measured and predicted standard deviations σ_r of shoreline oscillations

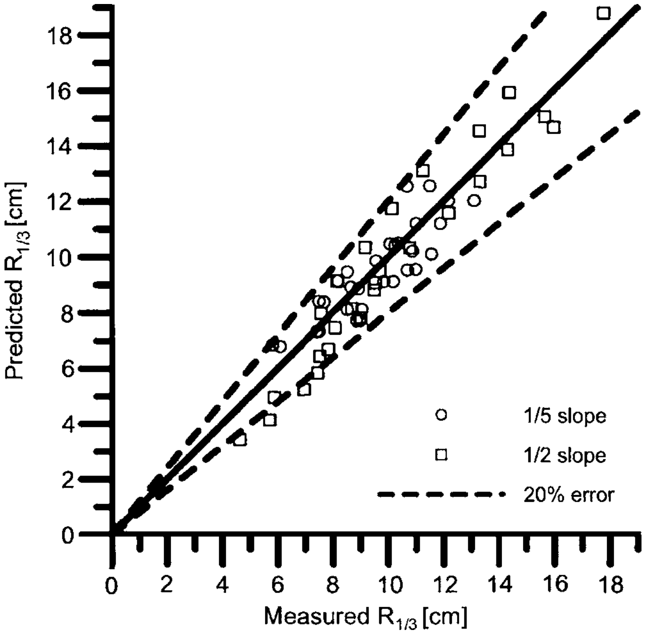

Fig. 12. Measured and predicted significant runup heights $R_{1/3}$

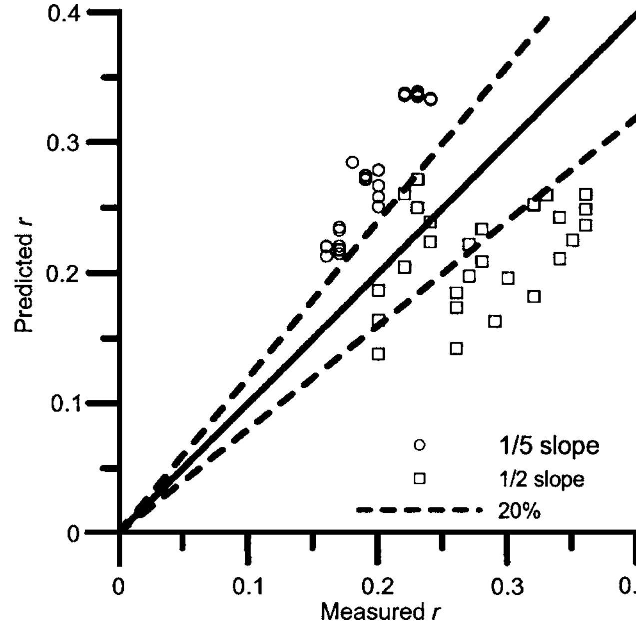

Fig. 14. Measured and predicted wave reflection coefficients r

$$\xi = \left(\frac{gT_p^2}{2\pi H_{1/3}}\right)^{0.5} \tan\theta; \quad \gamma_h = 1 - 0.03\left(4 - \frac{d_t}{H_{1/3}}\right)^2 \quad \text{if } \frac{d_t}{H_{1/3}} < 4 \tag{12}$$

where ξ=surf similarity parameter; $H_{1/3}$=significant wave height at the toe of the slope; γ_f=reduction factor due to slope roughness; and γ_h=reduction factor due to wave breaking on a shallow foreshore which is less than unity if $(d_t/H_{1/3})<4$. Eq. (11) implies that $(1.5\,\xi)$ is replaced by 3.0 if $\xi>2$. The reduction factor γ_h based on the measured ratio, $H_{2\%}/(1.4H_{1/3})$, on a foreshore slope of 1/100 with $H_{2\%}$=2% wave height is assumed to be valid for the present beach slopes of 1/34.4 and 1/32.1. The reduction factor γ_f for a rubble layer with two or more stone diameter thicknesses was suggested to be in the range of 0.50–0.55 for $\xi<4$ and larger for $\xi>4$ but γ_f=0.52 is used here to obtain the fair agreement shown in Fig. 13. The significant wave height $H_{1/3}$ for each test is obtained from the time series of the free surface elevation measured by the wave gauge at the toe of the slope. For the 1/5 slope tests, $0.97<\xi<2.23$ and $0.78<\gamma_f<0.91$. For the 1/2 slope tests, $2.85<\xi<9.33$ and $0.61<\gamma_f<0.86$. Eq. (11) developed originally for $0.5<\xi<5$ is applied here for $0.97<\xi<9.33$. Fig. 13 indicates that the numerical model and empirical formula predicts $R_{2\%}$ within the error of about 20%. It should be noted that the numerical model uses the measured H_{rms} outside the surf zone instead of the measured $H_{1/3}$ at the toe of the slope.

Finally, Fig. 14 compares the measured and predicted reflection coefficient r at x=0 where r is predicted using Eq. (6). The numerical model overpredicts r for the 1/5 slope and underpredicts r for the 1/2 slope. The wave reflection coefficient estimated from the residual wave energy flux at the still water shoreline may be crude but is useful in estimating the order of magnitude of wave reflection using the time-averaged model.

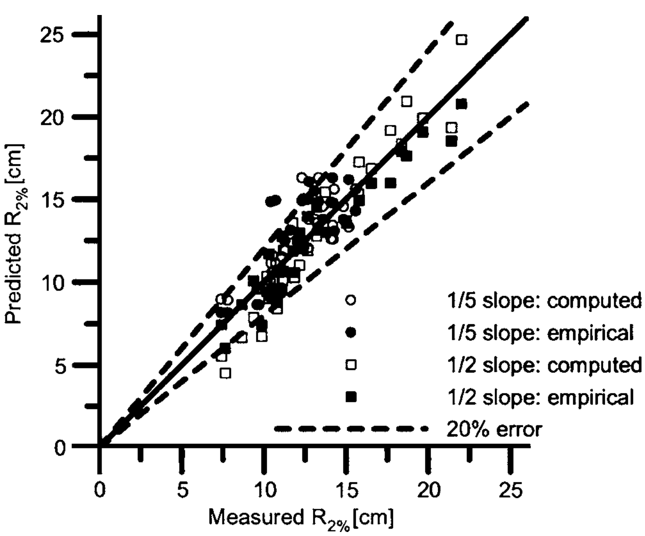

Fig. 13. Measured, computed, and empirical 2% runup heights $R_{2\%}$

Conclusions

The numerical model developed for the prediction of irregular breaking wave transmission over a submerged porous breakwater by Kobayashi et al. (2007) is extended to predict irregular wave shoaling and breaking on a beach with a gentle slope and irregular wave runup on a permeable slope that represents a cobble beach and a stone revetment. The numerical model based on the time-averaged continuity, momentum, and energy equations predicts the cross-shore variations of the mean and standard deviation of the free surface elevation and the horizontal velocities above and inside the permeable layer. The mean and standard deviation of the shoreline oscillations on the permeable slope are estimated using the predicted statistics of the free surface elevation as shown in Fig. 2. The probability distribution of individual runup heights above SWL is assumed to be given by the Rayleigh distribution where the effect of wave setup is included. The significant runup height is related empirically to the mean and standard deviation of the shoreline oscillations.

The developed model is compared with small-scale experiments with 1/5 and 1/2 slopes. The numerical model is shown to predict the cross-shore variations of the mean and standard deviation of the measured free surface elevation and horizontal velocity above the permeable slope fairly accurately when the breaker ratio parameter γ is calibrated for some of the 1/2 slope tests. No measurement was made of the velocity inside the permeable layer. The computed results with and without the permeable layer are compared to examine the degree of the permeability effects which are found to reduce the wave energy dissipation rate due to wave breaking. The numerical model predicts the mean and standard deviation of the measured shoreline oscillations reasonably well except that the mean is overpredicted for some of the 1/2 slope tests. Nevertheless, the numerical model predicts the significant and 2% runup heights within an error of about 20%. This accuracy is similar to the accuracy of available empirical formulas based on the known wave conditions at the toe of the permeable slope. The advantage of this numerical model is that it can predict the irregular wave transformation on a beach of arbitrary profile including a nearshore bar (Kobayashi et al. 2005). Furthermore, the numerical model may be applied to gentler permeable slopes for which the effect of wave setup is not negligible. This numerical model is computationally efficient with the computation time on the order of 1 s and easy to use because no numerical difficulty has been experienced in the region of very small water depth. However, the numerical model will need to be verified using large-scale laboratory data and field data.

Acknowledgments

This study was partially supported by the U.S. Army Corps of Engineers, Coastal and Hydraulics Laboratory under Contract No. DACW42-03-C-0024. The second writer was supported by a Scholarship from the Spanish Ministry of Education, F.P.U. No. AP20024082.

References

Battjes, J. A., and Stive, M. J. F. (1985). "Calibration and verification of a dissipation model for random breaking waves." *J. Geophys. Res.*, 90(C5), 9159–9167.

de los Santos, F. J., and Kobayashi, N. (2005). "Irregular wave setup and runup on cobble beaches and revetments." *Research Rep. No. CACR-05-06*, Center for Applied Coastal Research, Univ. of Delaware, Newark, Del.

de los Santos, F. J., Kobayashi, N., Meigs, L. E., and Losada, M. A. (2005). "Irregular wave runup on porous structures and cobble beaches." *Proc., Waves'2005 Conf.*, ASCE, Reston, Va., Paper No. 30, 1–10.

Goda, Y. (2000). *Random seas and design of maritime structures*, World Scientific, Singapore.

Johnson, B. D., and Kobayashi, N. (1998). "Nonlinear time-averaged model in surf and swash zones." *Coastal Engineering 1998, Proc., 26th Coastal Engineering Conf.*, ASCE, Reston, Va., 2785–2798.

Kearney, P. G., and Kobayashi, N. (2001a). "Irregular breaking wave transformation on a beach and runup on a revetment." *Research Rep. No. CACR-01-01*, Center for Applied Coastal Research, Univ. of Delaware, Newark, Del.

Kearney, P. G., and Kobayashi, N. (2001b). "Time-averaged probabilistic model for irregular wave runup on coastal structures." *Coastal Engineering 2000, Proc., 27th Coastal Engineering Conf.*, ASCE, Reston, Va., 2004–2017.

Kobayashi, N. (1999). "Wave runup and overtopping on beaches and coastal structures." *Advances in coastal and ocean engineering*, Vol. 5, World Scientific, Singapore, 95–154.

Kobayashi, N., Cox, D. T., and Wurjanto, A. (1990). "Irregular wave reflection and run-up on rough impermeable slopes." *J. Waterway, Port, Coastal, Ocean Eng.*, 116(6), 708–726.

Kobayashi, N., Herrman, M. N., Johnson, B. D., and Orzech, M. D. (1998). "Probability distribution of surface elevation in surf and swash zones." *J. Waterway, Port, Coastal, Ocean Eng.*, 124(3), 99–107.

Kobayashi, N., Meigs, L. E., Ota, T., and Melby, J. A. (2007). "Irregular breaking wave transmission over submerged porous breakwater." *J. Waterway, Port, Coastal, Ocean Eng.*, 133(2), 104–116.

Kobayashi, N., Otta, A. K., and Roy, I. (1987). "Wave reflection and runup on rough slopes." *J. Waterway, Port, Coastal, Ocean Eng.*, 113(3), 282–298.

Kobayashi, N., Zhao, H., and Tega, Y. (2005). "Suspended sand transport in surf zones." *J. Geophys. Res.*, 109, C03045.

Liu, P. L.-F., Lin, P., Chang, K.-A., and Sakakiyama, T. (1999). "Numerical modeling of wave interaction with porous structures." *J. Waterway, Port, Coastal, Ocean Eng.*, 125(6), 322–330.

van der Meer, J. A., and Janssen, P. F. M. (1995). "Wave run-up and wave overtopping at dikes." *Wave forces on inclined and vertical wall structures*, ASCE, Reston, Va., 1–27.

van der Meer, J. A., Petit, H. A. H., van der Bosch, P., Klopman, G., and Broekens, R. (1993). "Numerical simulation of wave motion on and in coastal structures." *Coastal Engineering 1992, Proc., 23rd Coastal Engineering Conf.*, ASCE, Reston, Va., 1772–1784.

van Gent, M. R. A. (1995). "Porous flow through rubble-mound material." *J. Waterway, Port, Coastal, Ocean Eng.*, 121(3), 176–181.

van Gent, M. R. A. (2001). "Wave runup on dikes with shallow foreshores." *J. Waterway, Port, Coastal, Ocean Eng.*, 127(5), 254–262.

Wurjanto, A., and Kobayashi, N. (1993). "Irregular wave reflection and runup on permeable slopes." *J. Waterway, Port, Coastal, Ocean Eng.*, 119(5), 537–557.